

# Geophysical Research Letters



## RESEARCH LETTER

10.1029/2019GL086187

### Key Points:

- Vibroseis seismic surveys used to map the ice shelf cavity beneath Ekström Ice Shelf in Antarctica
- Deep trough with transverse sills and overdeepenings provide evidence of past ice streaming and retreat
- Two ocean circulation regimes inferred in the shallow and deep parts of the cavity

### Supporting Information:

- Supporting Information S1

### Correspondence to:

E. C. Smith,  
emma.smith@awi.de

### Citation:



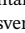



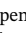

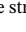


Smith, E. C., Hattermann, T., Kuhn, G., Gaedicke, C., Berger, S., Drews, R., et al. (2020). Detailed seismic bathymetry beneath Ekström Ice Shelf, Antarctica: Implications for glacial history and ice-ocean interaction. *Geophysical Research Letters*, 47, e2019GL086187. <https://doi.org/10.1029/2019GL086187>

Received 12 NOV 2019

Accepted 6 APR 2020

Accepted article online 3 MAY 2020

## Detailed Seismic Bathymetry Beneath Ekström Ice Shelf, Antarctica: Implications for Glacial History and Ice-Ocean Interaction

Emma C. Smith<sup>1</sup> , Tore Hattermann<sup>2</sup> , Gerhard Kuhn<sup>1</sup> , Christoph Gaedicke<sup>3</sup>, Sophie Berger<sup>1</sup> , Reinhard Drews<sup>4</sup> , Todd A. Ehlers<sup>4</sup> , Dieter Franke<sup>3</sup> , Rapahel Gromig<sup>1,5</sup> , Coen Hofstede<sup>1</sup> , Astrid Lambrecht<sup>6</sup>, Andreas Läufer<sup>3</sup> , Christoph Mayer<sup>6</sup> , Ralf Tiedemann<sup>1,7</sup> , Frank Wilhelms<sup>1,8</sup> , and Olaf Eisen<sup>1,7</sup> 

<sup>1</sup>Alfred-Wegener-Institut Helmholtz-Zentrum für Polar- und Meeresforschung, Bremerhaven, Germany, <sup>2</sup>Norwegian Polar Institute, Tromsø, Norway, <sup>3</sup>BGR, Federal Institute for Geosciences and Natural Resources, Hannover, Germany, <sup>4</sup>Department of Geosciences, University of Tübingen, Tübingen, Germany, <sup>5</sup>Now at Institute of Geology and Mineralogy, University of Cologne, Cologne, Germany, <sup>6</sup>Geodesy and Glaciology, Bavarian Academy of Sciences and Humanities, Munich, Germany, <sup>7</sup>Department of Geosciences, University of Bremen, Bremen, Germany, <sup>8</sup>Department of Geosciences, University of Göttingen, Göttingen, Germany

**Abstract** The shape of ice shelf cavities are a major source of uncertainty in understanding ice-ocean interactions. This limits assessments of the response of the Antarctic ice sheets to climate change. Here we use vibroseis seismic reflection surveys to map the bathymetry beneath the Ekström Ice Shelf, Dronning Maud Land. The new bathymetry reveals an inland-sloping trough, reaching depths of 1,100 m below sea level, near the current grounding line, which we attribute to erosion by palaeo-ice streams. The trough does not cross-cut the outer parts of the continental shelf. Conductivity-temperature-depth profiles within the ice shelf cavity reveal the presence of cold water at shallower depths and tidal mixing at the ice shelf margins. It is unknown if warm water can access the trough. The new bathymetry is thought to be representative of many ice shelves in Dronning Maud Land, which together regulate the ice loss from a substantial area of East Antarctica.

**Plain Language Summary** Antarctica is surrounded by floating ice shelves, which play a crucial role in regulating the flow of ice from the continent into the oceans. The ice shelves are susceptible to melting from warm ocean waters beneath them. In order to better understand the melting, knowledge of the shape and depth of the ocean cavity beneath ice shelves is crucial. In this study, we present new measurements of the sea floor depth beneath Ekström Ice Shelf in East Antarctica. The measurements reveal a much deeper sea floor than previously known. We discuss the implications of this for access of warm ocean waters, which can melt the base of the ice shelf and discuss how the observed sea floor features were formed by historical ice flow regimes. Although Ekström Ice Shelf is relatively small, the geometry described here is thought to be representative of the topography beneath many ice shelves in this region, which together regulate the ice loss from a substantial area of East Antarctica.

## 1. Introduction

Ice shelves surrounding Antarctica act as buttresses, restraining ice discharge from the continent into the oceans, and therefore regulating Antarctic contributions to sea level rise (Dupont & Alley, 2005). Mass loss from Antarctica has been accelerating over the past 20 years (IPCC, 2019), driven by increased basal melting of ice shelves (Paolo et al., 2015; Pritchard et al., 2012). Accurate knowledge of the geometry of the ice shelf cavities and the properties of the water column beneath them are essential for understanding processes active at the ice shelf ocean interface. Recent studies have highlighted a lack of sub-ice-shelf bathymetry as a “major limitation” (Pattyn et al., 2017) for future projections of Antarctic mass balance. Improved bathymetric mapping allows determination of water access pathways and calculation of spatially and temporally variable melt rates (e.g., Cochran et al., 2014; Goldberg et al., 2019; Milillo et al., 2019; Morlighem et al., 2020; Pattyn et al., 2017; Tinto et al., 2019). In addition, sub-ice-shelf bathymetry also provides information about ice dynamic history. Understanding past ice dynamics and implementing an accurate bathymetry in ice-flow and oceanographic models, is a critical step to improve projections of the evolution of the ice sheets.

©2020. The Authors.

This is an open access article under the terms of the Creative Commons Attribution License, which permits use, distribution and reproduction in any medium, provided the original work is properly cited.

The coast of Dronning Maud Land (DML), East Antarctica (Figure 1) is fringed by numerous small ice shelves. In this area, satellite-derived melt rates are typically low (Rignot et al., 2013). However, the continental shelf is narrow (Figure 1b), meaning the ice shelves of DML are in close proximity to Warm Deep Water (WDW) masses which flow along the continental slope, making this a potentially sensitive region to future change (Hattermann, 2018; Heywood et al., 2013; Thompson et al., 2018). It has also been highlighted as susceptible to marine ice sheet instability (Morlighem et al., 2020; Ritz et al., 2015). In addition, the ice shelf-ocean interactions along the DML coast play an important role in preconditioning the structure and water mass properties of the westward flowing boundary current (Fahrbach et al., 1994; Hattermann, 2018). This current is a key control on warm-water inflow toward the Filchner-Ronne Ice Shelf (Hellmer et al., 2017; Timmermann & Hellmer, 2013) and bottom water formation in the southern Weddell Sea (Meijers et al., 2016; Meredith et al., 2011). The few bathymetric measurements that exist under DML ice shelves have revealed cavities that are much deeper than those included in current gridded data sets of Antarctica (e.g., Fretwell et al., 2013; Morlighem et al., 2020). Under the Fimbul Ice Shelf (Figure 1b), a deep trough within the subshelf cavity was discovered (Nøst, 2004) and confirmed to contain modified WDW (Hattermann et al., 2012, 2014). At the front of the Roi Baudouin Ice Shelf, in eastern DML, an 850-m-deep trough is present, which has major consequences when simulating ice sheet advance and retreat (Berger, 2017; Favier et al., 2016). This emerging picture highlights the need for more accurate bathymetry measurements in this region.

The general lack of bathymetry measurements beneath ice shelves is the result of difficulties in access: radar systems do not penetrate through the water column; gravity inversions are possible, but without control points are sensitive to assumptions about the underlying geology (Eisermann et al., 2020); drilling through the ice provides limited spatial range and is logistically challenging; and the use of autonomous underwater vehicles is rare, as they require ship support (e.g., Jenkins et al., 2010; Nicholls et al., 2006). Seismic surveys currently provide the most reliable method to map water column thickness, as well as to image the sea bed below.

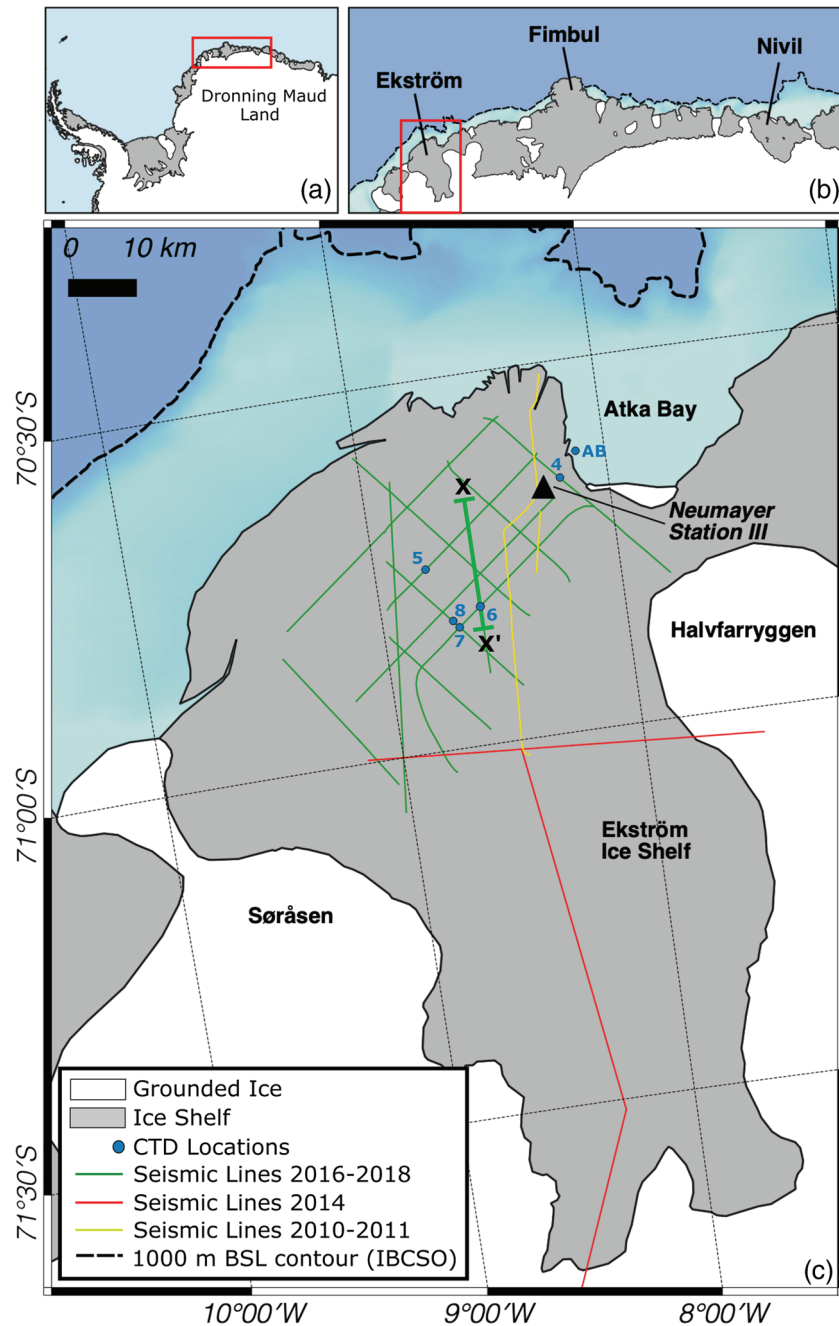
Here we address this problem using a specialized vibroseis seismic source and snow streamer system (Eisen et al., 2015) to create a new map of the ice shelf cavity and sea floor bathymetry beneath the Ekström Ice Shelf, DML. Ekström Ice Shelf (Figure 1) covers an area of approximately 6,800 km<sup>2</sup> with basal melt rates of up to 1.1 ma<sup>-1</sup> (Neckel et al., 2012). It is laterally constrained by the grounded ice rises of Søråsen to the west and Halvfarryggen in the east (Figure 1c). The present ice shelf front is less than 20 km from the continental shelf break. Until now, little was known about the bottom topography of the ice-shelf cavity. A number of seismic reflection measurements by Kobarg (1988) suggest a southward deepening of the sea floor with a maximum water column thickness of 500 m. However, a map of the cavity is currently lacking. We integrate our bathymetric mapping with conductivity-temperature-depth (CTD) data acquired through hot water drilled access holes in the ice shelf and under sea ice in Atka Bay (Figure 1c). The combined observations are used to identify the primary implications of this new bathymetry for ice-ocean interaction and ice dynamic history in the region. They show the urgent need for more measurements of sub-ice-shelf bathymetry along the coast of this sector of Antarctica and for many other ice shelves, where the bathymetry is equally poorly constrained.

## 2. Data and Methods

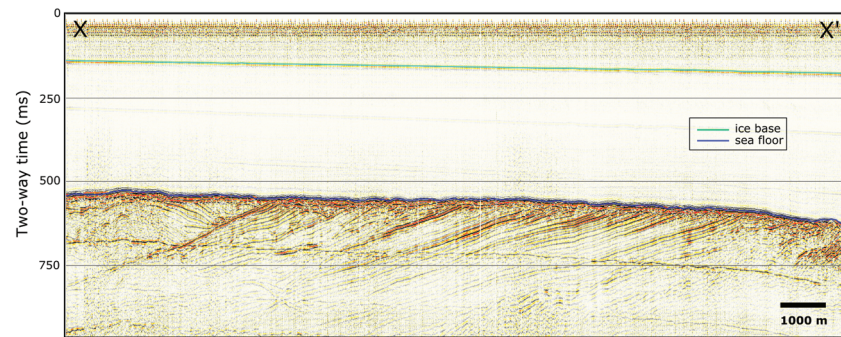
### 2.1. Seismic Data Acquisition

Seismic data were collected between 2010 and 2018, using two different vibroseis seismic sources. The snow streamer, used for all data acquisition, was 1,500 m long, containing 60 channels, with a 25-m group spacing. Each group contained eight gimbaled P-wave SM-4, 14-Hz geophones. For all data collection the vibroseis source was towed behind a snow tractor with the snow streamer towed behind that. This method of operation allowed for data acquisition rates of up to 20 km per day for ten fold data. Fold refers to the amount of times a subsurface point (referred to as a common midpoint, CMP) is sampled by different source/receiver pairs. A more detailed explanation of both these seismic sources, the snow streamer, and the operational method is given in Eisen et al. (2015).

The main grid of data, at the ice shelf front, was collected during the 2016/2017 and 2017/2018 austral summers (Figure 1c, green) as part of the Sub-EIS-Obs project (Kuhn & Gaedicke, 2015). The seismic source was the AWI IVI EnviroVibe, producing a 10-s linear sweep from 10 to 220 Hz. These data are relatively high fold (6–15), with the exception of the two lines in the north-western corner of the grid, which are single



**Figure 1.** (a) Location of Dronning Maud Land within Antarctica (b) Area highlighted in (a) with location of Ekström Ice Shelf indicated and (c) Ekström Ice Shelf with seismic survey lines and conductivity-temperature-depth (CTD) locations shown. In all figures the ice shelf is shown in gray and grounded ice in white. In (b) and (c) the ocean background is from the International Bathymetric Chart of the Southern Ocean (IBCSO) (Arndt et al., 2013), with the 1,000 m below sea level (BSL) contour shown as a dashed line, indicating the location of the continental slope. The CTD location labels “4” to “8” refer to hot water drilled access holes “EIS-4” to “EIS-8” and “AB” to the location of a sea ice lead in Atka Bay. The location of the seismic line shown in Figure 2 is X-X’.



**Figure 2.** Example of a seismic time-stacked section. Location of section is marked X–X' in Figure 1, AWI line number 20170561. Reflections from the ice shelf base and sea floor are clearly visible, and the TWT to them can be easily determined. The section is vertically exaggerated by a factor of 10.

fold. It was not possible to extend data collection further west due to surface crevassing. The seismic lines extending across the grounding line to the east and south were collected in 2014 (Figure 1c, red), using the same acquisition configuration, and are single fold. Three older lines from 2010 and 2011 overlap the main grid (Figure 1c, yellow) and were acquired using the University of Bergen Failing Y-1100 vibroseis source (Kristoffersen et al., 2014), with a 10-s sweep from 10 to 100 Hz; fold varies between one and eight.

All seismic data were processed specifically for this study to ensure consistent treatment of data from different surveys (supporting information, Text S1). The resulting seismic time-stacked sections all have clear ice base and the sea floor reflections (Figure 2). The two-way traveltimes (TWTs) of these reflections were handpicked on each section.

## 2.2. Depth Conversion and Gridding of Seismic Measurements

The handpicked TWTs from all seismic lines were used to create grids of the TWT to the ice base and sea floor, using a kriging algorithm. Any misties between picks, in areas where seismic lines overlap, were handled by assigning priority to the higher resolution surveys. Each grid was then depth converted using a seismic velocity of  $3,601 \text{ ms}^{-1}$  for the ice shelf and  $1,451 \text{ ms}^{-1}$  for the water column (supporting information, Text S2). The final step was to correct the depth of each grid for the ice surface elevation, using the REMA digital elevation model v1.1 (Howat et al., 2019), which was rereferenced to the GL04C geoid (Förste et al., 2008).

## 2.3. Uncertainties in Seismic Depths

Uncertainties in the sea floor depth, from seismic measurements, come from four main sources: (i) accuracy of the horizon picking, (ii) velocities used for depth conversion of these horizons, (iii) errors in the REMA DEM used for surface elevation corrections, and (iv) depth errors from unmigrated data. A detailed analysis of these individual error sources was made (supporting information, Text S3), resulting in cumulative error at the sea floor of  $\pm 14.8 \text{ m}$  in the area of the main data grid and  $\pm 34.4 \text{ m}$  in the areas of the 2014 seismic lines, which extend from the main grid toward the grounding lines (Figure 1). The gridded bathymetry may have larger errors away from the seismic lines.

It was possible to measure the ice thickness and sea floor depth at the five hot water drilled access hole locations (4–8; Figure 1) on the ice shelf, both during drilling and with camera equipment and coring devices deployed through the holes to the sea floor. These measurements confirmed that the seismic determined ice thickness was within  $\pm 5 \text{ m}$  of the measured thickness and the sea floor within  $\pm 10\text{--}20 \text{ m}$ . This validates our error estimates, as the latter range also includes horizontal displacement of the sampling rope by ocean currents.

## 2.4. CTD Data

During the 2018/2019 austral summer, hot water drilled access holes were made at five locations on the ice shelf (4–8; Figure 1). An RBR Concerto CTD sensor was repeatedly lowered through each hole and additionally through a sea ice lead in Atka Bay (AB; Figure 1), giving a total of six CTD measurement sites. The CTD sensor recorded water mass properties at a frequency of 1 Hz (vertical resolution of 0.5–2 m), from which pressure, in situ temperature, and practical salinity data were extracted (supporting information, Text S4). The uncertainty for in situ temperature is  $0.02^\circ \text{C}$  and for practical salinity 0.03. These data were used to

calculate seismic velocities for depth conversion of the sea floor seismic reflection (supporting information, Text S2) and to investigate water masses present beneath the ice shelf and sea ice.

### 3. Results and Discussion

The new sub-ice-shelf bathymetry (Figure 3a) is independent of any previously available products of ice thickness and water depth. Here, we compare the new bathymetry to the Bedmap2 (Fretwell et al., 2013) Antarctic bed topography (Figure 3b), which has been the baseline Antarctic dataset for the large majority of modeling studies. We highlight the differences to emphasize the need for dedicated measurements of sub-ice-shelf bathymetry.

Given the lack of previously available data, the Bedmap2 (Fretwell et al., 2013) sea floor bathymetry beneath Ekström Ice Shelf closely follows the ice base topography, deepening toward the grounding line. This suggesting a relatively thin, uniform water column height of the ice shelf cavity (Figure 3b). The new seismic bathymetry, in contrast, reveals a much more distinct geometry of the ice shelf cavity (Figure 3c). Similar mismatches have been documented for other ice shelves in this sector (e.g., Nøst, 2004).

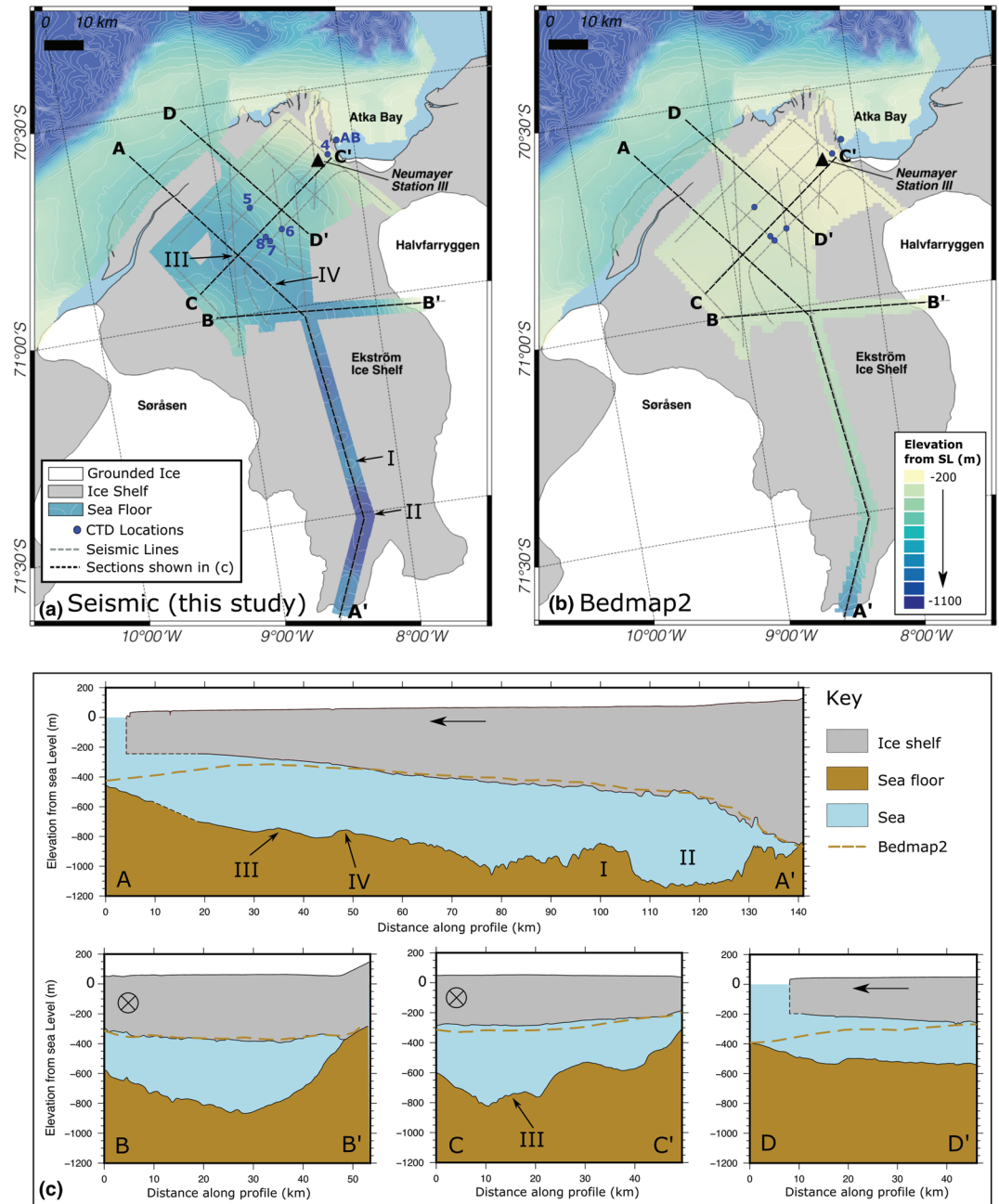
Beneath the main grid of our data (Figure 3a) we find a bathymetric trough under the central part of the ice shelf, which appears to be aligned with the current ice flow direction. In this area the trough is 30 km wide and reaches depths of up to 800 m below sea level (Figures 3a and 3c, C–C'). The trough flanks have depths around 450–500 m (Figures 3a and 3c, C–C' and D–D'), shallowing to around 300 m depth at the marginal grounding line joining the ice shelf to the ice rise of Halvfarryggen (Figures 3a and 3c, B–B'). Shallowing topography is also seen toward the western grounding line at Søråsen, and it is likely this mirrors the cavity shape to the east. The sea floor directly in front of the ice shelf is 450 m deep, similar to the flanks of the trough. A basin-like depression, around 570 m deep, is seen on the eastern plateau to the south of Neumayer Station III. The profile from the front of the ice shelf edge to the current grounding line (Figures 3a and 3c, A–A') follows the axis of the trough under the main grid and the single seismic line connecting the south of the grid to the grounding line. This indicates an inland-sloping sea floor (Figures 3a and 3c, A–A'), reaching a maximum depth of 1,100 m around 10-km seaward of the current grounding line.

#### 3.1. Ice Dynamic History

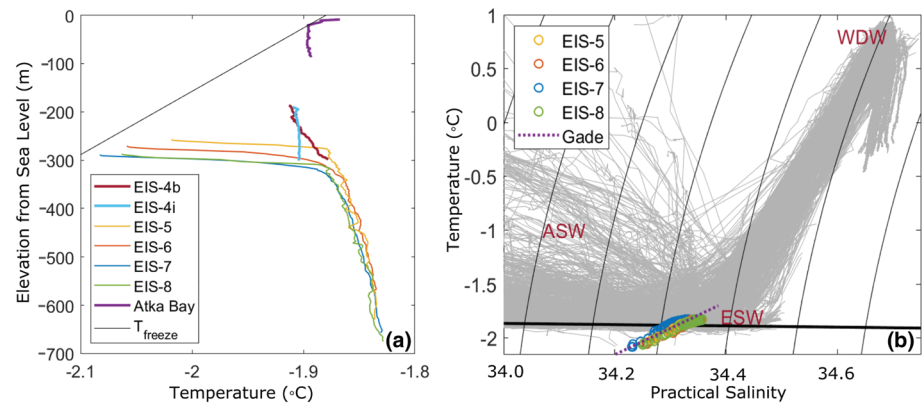
The sea-floor bathymetry under Ekström Ice Shelf allows us to interpret features associated with past ice sheet configurations in this region. The deepened trough under the center of the ice shelf (Figure 3a) is interpreted as a relict landscape, formed through erosion by former ice streams. The flanks of the trough and the sea floor at the ice-shelf front are around 300–400 m shallower than the trough. The trough does not cross-cut the outer parts of continental shelf, and it is therefore likely that the seaward rising continental shelf was a previous grounding line.

Sediment core records in front of Ekström Ice Shelf are sparse (Grobe & Mackensen, 1992; Hillenbrand et al., 2014) and do not provide conclusive evidence as to whether grounded ice covered the entire continental shelf, as far as the continental slope (approximately the 1,000-m contour in Figure 1), during the Last Glacial Maximum (LGM: 23–19 ka BP). Sediment cores from the continental shelf, in front of Ekström Ice Shelf, were not deep enough to penetrate into material from the LGM. The recovered Holocene aged sediments (11.7 ka BP to present), were likely deposited beneath an ice shelf (Grobe & Mackensen, 1992), close to the grounding line. Our finding that the trough does not cross-cut the outer parts of continental shelf suggests that grounded ice likely reached to the inner parts of the continental shelf (around the current ice-shelf front) in the past, possibly at the LGM, but the precise grounding line position remains unresolved.

The seismic line extending from the main grid to the south (Figure 3c, A–A') shows a sea floor that deepens toward the current grounding line. The general trend of a retrograde slope within the trough would likely have put this area at risk of rapid ice retreat after the LGM, until a stable grounding line position (e.g., a topographic high) was reached. There are a number of topographic highs along the ice flow direction. Particularly prominent is the topographic high at 100 km along profile A–A' (I; Figure 3c), which is around 200 m above the surrounding sea floor. We suggest that this is a former grounding line position, given its significant elevation. However, current bathymetry measurements in this region do not extend laterally to confirm the extent of this feature. There is a significant overdeepening upstream of this high (II; Figure 3c), reaching 1,100 m depth around 10-km seaward of the current grounding line. Overdeepenings are commonly formed in areas of convergent ice stream flow, where ice velocities and erosional potential are high



**Figure 3.** (a) Gridded sea floor bathymetry beneath the Ekström Ice Shelf, derived from seismic measurements (this study). (b) The same area as (a) but with subice shelf bathymetry from Bedmap2 (Fretwell et al., 2013) co-located with the seismic bathymetry. In both (a) and (b) bathymetry seawards of the ice shelf edge is from the International Bathymetric Chart of the Southern Ocean (IBCSO) (Arndt et al., 2013) mapping project and is cut to the area where measurements are present, note that ice shelf front was further landward than present day when some measurements were made. White contours are at 50-m intervals. Features I–IV are indicated (see text for details). Gray dashed lines show the seismic data locations, with the cross sections shown in (c) indicated by black dashed lines. Blue points indicate the location of conductivity-temperature-depth (CTD) measurements, as in Figure 1. (c) Cross sections of the ice shelf cavity and sea floor beneath and in front of Ekström Ice Shelf. Ice flow direction is indicated by arrows and cross hairs. Sea floor bathymetry (brown) is from the seismic grid merged with IBSCO, seaward of the ice shelf edge. The ice shelf (gray) is derived from gridded seismic data at the ice base and REMA surface elevation. Solid black outlines are areas where data are present, dashed black lines in A–A' and D–D' are data gaps. Bedmap2 elevations are shown as brown dashed lines for comparison. All data are referenced to the GL04C geoid.



**Figure 4.** Vertical conductivity-temperature-depth (CTD) profiles taken through hot water drilled access holes (4–8; Figure 3a) and a sea ice lead (AB; Figure 3a). (a) In situ temperature observed at different sites beneath Ekström Ice Shelf and beneath sea ice in Atka Bay. Black line indicates the pressure-dependent melting point temperature for a given practical salinity of 34.25. (b) Distribution of in situ temperature and practical salinity profiles at the sites where reliable salinity measurements could be obtained. Gray profiles show the regional subset of open ocean CTD profiles presented in Hattermann (2018), indicating ambient water masses with abbreviations indicating the end members of Warm Deep Water (WDW), Eastern Shelf Water (ESW), and Antarctic Surface Water (ASW). The dashed purple line is the melt water mixing line along which a given water mass may transform through interaction with the ice shelf (Gade, 1979) when assuming zero conductive heat flux into the ice. Black curves indicate horizons of constant density, the thick near-horizontal black line indicates the melting point temperature at atmospheric pressure.

(Patton et al., 2016). The location of this overdeepening is at the convergence of two tributary glaciers, with higher modern-day ice flow velocities than the surrounding ice (Neckel et al., 2012). When ice was thicker and grounded further seaward, the overdeepened area would have been at the junction between these two tributaries, eroding the deep basin. Overdeepenings typically terminate in sills (Benn & Evans, 2014), where ice flow becomes less constrained, which could explain the origin of the topographic high we observe at 100 km along profile A–A'. Two smaller topographic highs at 35 km (III; Figure 3c) and 45 km (IV; Figure 3c) along profile A–A' are around 50 m in height, each separated by deeper basin areas, indicative of ice having been grounded at these points for some time.

A deep central trough punctuated with transverse topographic highs has also been observed under the neighboring Fimbul Ice Shelf (Nøst, 2004) and along the adjacent Coats Land ice margin (Hodgson et al., 2018, 2019). Under the front of Roi Baudouin Ice Shelf, eastern DML, an 850-m-deep trough (Berger, 2017; Favier et al., 2016) is present, hinting that this may also extend under the ice shelf in a similar way. This emerging picture suggests such deep troughs are ubiquitous in this sector of East Antarctica, indicating ice streams were a prevalent feature in the past and supporting the need for more widespread sub-ice-shelf bathymetry measurements.

### 3.2. Ice-Ocean Interaction

The implications for ice-ocean interactions in the Ekström region, from the newly mapped ice shelf cavity, refine our understanding of the role of DML ice shelves in the mass balance of the Antarctic ice sheets. Along this sector of the Antarctic coast, WDW masses are suppressed below the continental shelf break (Heywood et al., 2013) by the prevailing easterly winds in the “fresh shelf” regime (Thompson et al., 2018) that extends from about 20° W to 30° E. The sub-ice-shelf CTD profiles (Figure 4) confirm this, underpinning the relatively low basal melt rate estimates (Neckel et al., 2012) for the Ekström Ice Shelf. Most of the cavity is filled with relatively cold Eastern Shelf Water (ESW) that resides above the WDW along the DML coast (Nøst et al., 2011). In situ temperatures are close to the surface freezing point around  $-1.9^{\circ}\text{C}$  and practical salinity around 34.4. Only the upper tens of meters of the individual profiles show colder (Figure 4a), less saline water masses, indicating buoyant outflows of Ice Shelf Water in a surface layer near the ice shelf base that is aligned along common melt water mixing line (Figure 4b, Gade, 1979) originating from the ESW.

Although the deeper trough beneath the central part of the ice shelf does not cross-cut the continental shelf break, it provides a possible conduit for warmer inflows reaching onto the continental shelf to enter the ice-shelf cavity (Figure 3c, A–A'). Intermittent, warmer near-bottom inflows have been observed across a slightly deeper sill beneath the neighboring Fimbul Ice Shelf (Hattermann et al., 2012) and a rise of WDW

along the DML coast has been suggested as a possible response to future climate change (Hattermann, 2018; Hellmer et al., 2017). In these scenarios, the newly revealed several hundred meters of water depth of the Ekström cavity would support a cavity overturning circulation, where warm near-bottom inflows can propagate undiluted toward the grounding line, rendering Ekström Ice Shelf more vulnerable to warm inflows than implied by previous bathymetric datasets. Our example is also likely to be instructive for many smaller, unmapped ice shelves that have a similar configuration and glacial history along the DML coast and elsewhere.

The presence of extensive ocean cavities beneath Ekström and potentially other DML ice shelves has implications for the susceptibility to local marine ice sheet instability (Morlighem et al., 2020; Ritz et al., 2015), as well as for far field effects through melt induced altering water mass properties of the westward boundary current. While ice shelf melt water presently contributes little to the freshening of the ESW (Zhou et al., 2014), there is growing evidence that basal melting feedbacks play an important role for the slope front overturning that controls the depth of the thermocline at the shelf break (e.g., Hattermann, 2018). This regulates the access of warm water to the vast Filchner-Ronne Ice Shelf in the southern Weddell Sea (e.g., Hellmer et al., 2017). A correct representation of warm water pathways to the ice shelves upstream of the Filchner Trough will hence be crucial to quantifying these effects and assessing the uncertainty of model projections.

Locally, our observed seafloor bathymetry suggests a separation of different circulation regimes beneath the ice shelf. While the central part of the cavity seems to be dominated by the trough system; the eastern portion of the ice shelf, adjacent to Atka Bay, comprises a relatively shallow water column (Figures 3a and 3c, C–C') that is likely subject to intense tidal mixing and may be responsible for the vigorous accretion of marine ice in the area (Arndt et al., 2020). The two successive temperature profiles from the EIS-4 site confirm the existence of a tidally mixed zone in this region. While the EIS-4b profile shows a similar vertical gradient in temperature to the profiles obtained in the deeper part of the cavity, the EIS-4i profile has a more homogeneous vertical temperature structure. The EIS-4i profile was taken about 11 hours later than EIS-4b, and according to the CATS regional tidal model (Padman et al., 2008), a relatively large amplitude tidal wave passed the EIS-4 hole location between the two measurements. Hoppmann et al. (2015) found that platelet ice crystals leave the ice-shelf cavity in intermittent pulses at this location, and similar tidal flushing events may be responsible for mixing larger volumes of potentially supercooled Ice Shelf Water in shallower depths, contributing to the platelet ice formation under the fast ice in Atka Bay that has been identified as a prominent habitat in the sea ice ecosystem (e.g., Smetacek et al., 1992). A recent study also shows that propagating tidal waves may play an important role in modulating basal melting near the ice shelf grounding lines (Sun et al., 2019), further emphasizing the need for knowledge of the local cavity shape to assess and interpret the melt rate variability of a given region.

#### 4. Conclusions

We have presented new bathymetry data from under the Ekström Ice Shelf, Dronning Maud Land, Antarctica. The use of vibroseis seismic reflection surveys proves an effective method for collecting high-resolution data across large areas of the ice shelf. As a result, the Ekström Ice Shelf cavity is currently one of the best mapped in Antarctica. The discovery of a deep trough with transverse sills under Ekström Ice Shelf is the second example of such a feature under a DML ice shelf, after the neighboring Fimbul Ice Shelf, with similar features also found along the adjacent Coats Land margin (Hodgson et al., 2018, 2019) and at the ice shelf front of Roi Baudouin (Berger, 2017; Favier et al., 2016). This growing list of evidence suggests that the bathymetry we see at Ekström, Fimbul, and along the Coats Land coast is likely characteristic of other ice shelves in the DML and neighboring regions. While these ice shelves are small, they are numerous and very little is known about the cavity geometry, which is a fundamental gap in our ability to understand past ice dynamics and future stability of this region. The ice shelves of DML are known to play a key role in preconditioning the water mass properties of the westward flowing boundary current, which affects the much larger Filchner-Ronne Ice Shelf and thus large portions of the West Antarctica Ice Sheet. Improved knowledge of ice shelf cavities is a key required step toward better understanding and projections of the fate of marine ice sheets in a warming climate.

#### Author Contributions

All authors contributed to seismic target and profiling design, discussed the manuscript, and contributed comments toward the final version. ECS designed and wrote the paper, performed fieldwork, and led one



field season, analyzed, and interpreted seismic data; TH analyzed CTD data and provided the oceanographic component to the paper; DF and A Lambrecht performed seismic data acquisition and analysis; CM performed seismic data acquisition and led one field season; SB acquired and analyzed CTD data and provided glaciological constrains for ice shelf processes; RD, TAE, and CM contributed ice flow modeling results and glaciological/geological constraints for data interpretation; CH was in charge of the seismic equipment and processed seismic data; GK, CG, A Läufer, and RT provided geological constraints for data interpretation; FW prepared and coordinated the hot water drilling system; RG led one field season and performed cavity sampling; OE coordinated and implemented the seismic field work, led three field seasons, performed seismic and CTD data acquisition. GK, CG, A Läufer, RT, FW, and OE are project Co-PIs, designed financial support and project implementation; CG and OE administratively coordinated the project. The transdisciplinary science component is based on Kuhn and Gaedicke (2015).

### Acknowledgments

Field work and data processing by ECS since 2016 were funded through the AWI-BGR Sub-EIS-Obs Project. ECS was additionally funded through the DFG Cost S2S project Grant EI672/10-1 in the framework of the priority program “Antarctic Research with comparative investigations in Arctic ice areas,” RD by the Grants MA 3347/10-1, EH 329/13-1, and DR 822/3-1. The field work of A. Lambrecht in 2010 was kindly supported by the Institute of Meteorology and Geophysics, University of Innsbruck, Austria. SB was partly funded by the MIMO (Monitoring melt where Ice Meets Ocean) project, Belgian Science Policy Contract SR/00/336. We thank R. Blenkner, J. Köhler, H. Schubert, J. Tell, B. Ehlers, S. Hilmarrsson, and the staff at Neumayer Station III for logistical and other support. N. Koglin for discussion on hot water drilled access hole locations and geological constraints. The authors would like to thank C. Haas and J-L. Tison for loan on the CTD equipment, D. Hodgson, and one anonymous reviewer for constructive and detailed feedback and Emerson E&P Software, Emerson Automation Solutions, for providing licenses for the seismic software Paradigm, in the scope of the Emerson Academic Program. The initial idea for envisaging a geologic drilling underneath Ekström Ice Shelf was put forward by Y. Kristoffersen, who’s stimulating creativity and technical support over the years the authors would like to acknowledge in particular. Data presented in this study are archived with PANGAEA and are freely available at the following locations: gridded sea-floor bathymetry data (<https://doi.org/10.1594/PANGAEA.907951>) and raw CTD data (<https://doi.org/10.1594/PANGAEA.914478>).

### References

- Arndt, S., Hoppmann, M., Schmithüsen, H., Fraser, A. D., & Nicolaus, M. (2020). Seasonal and interannual variability of landfast sea ice in Atka Bay, Weddell Sea, Antarctica. *The Cryosphere Discussions*, 1–26. <https://doi.org/10.5194/tc-2019-293>
- Arndt, J. E., Schenke, H. W., Jakobsson, M., Nitsche, F. O., Buys, G., Goleby, B., et al. (2013). The International Bathymetric Chart of the Southern Ocean (IBCSO) Version 1.0—A new bathymetric compilation covering circum-Antarctic waters. *Geophysical Research Letters*, 40, 3111–3117. <https://doi.org/10.1002/GRL.50413>
- Benn, D., & Evans, D. J. A. (2014). Erosional processes, forms and landscapes, (2nd ed.), *Glaciers and Glaciation* pp. 816): Routlage.
- Berger, S. (2017). Stability of Antarctic ice shelves—A case study of Roi Baudoin Ice Shelf, Dronning Maud Land, East Antarctica (PhD).
- Cochran, J. R., Jacobs, S. S., Tinto, K. J., & Bell, R. E. (2014). Bathymetric and oceanic controls on Abbot Ice Shelf thickness and stability. *The Cryosphere*, 8(3), 877–889. <https://doi.org/10.5194/tc-8-877-2014>
- Dupont, T. K., & Alley, R. B. (2005). Assessment of the importance of ice-shelf buttressing to ice-sheet flow. *Geophysical Research Letters*, 32, L04503. <https://doi.org/10.1029/2004GL022024>
- Eisen, O., Hofstede, C., Diez, A., Kristoffersen, Y., Lambrecht, A., Mayer, C., et al. (2015). On-ice vibroseis and snowstreamer systems for geoscientific research. *Polar Science*, 9(1), 51–65. <https://doi.org/10.1016/j.polar.2014.10.003>
- Eisermann, H., Eagles, G., Ruppel, A., Smith, E. C., Jokat, W., & Resources, N. (2020). Bathymetry beneath ice shelves of western Dronning Maud Land, East Antarctica, and implications on ice shelf stability. *Geophysical Research Letters*, 47. <https://doi.org/10.1029/2019GL086724>
- Fahrbach, E., Rohardt, G., Schröder, M., & Strass, V. (1994). Transport and structure of the Weddell Gyre. *Annales Geophysicae*, 12(9), 840–855. <https://doi.org/10.1007/s00585-994-0840-7>
- Favier, L., Pattyn, F., Berger, S., & Drews, R. (2016). Dynamic influence of pinning points on marine ice-sheet stability: A numerical study in Dronning Maud Land, East Antarctica. *The Cryosphere*, 10(6), 2623–2635. <https://doi.org/10.5194/tc-10-2623-2016>
- Förste, C., Schmidt, R., Stubenvoll, R., Flechtner, F., Meyer, U., König, R., et al. (2008). The GeoForschungsZentrum Potsdam/Groupe de Recherche de Géodésie Spatiale satellite-only and combined gravity field models: EIGEN-GL04S1 and EIGEN-GL04C. *Journal of Geodesy*, 82(6), 331–346. <https://doi.org/10.1007/s00190-007-0183-8>
- Fretwell, P., Pritchard, H. D., Vaughan, D. G., Bamber, J. L., Barrand, N. E., Bell, R., et al. (2013). Bedmap2: Improved ice bed, surface and thickness datasets for Antarctica. *The Cryosphere*, 7(1), 375–393. <https://doi.org/10.5194/tc-7-375-2013>
- Gade, H. G. (1979). Melting of ice in sea water: A primitive model with application to the Antarctic ice shelf and icebergs. *Journal of Physical Oceanography*, 9(1), 189–198. [https://doi.org/10.1175/1520-0485\(1979\)009h0189:MOHSIW2.0.CO;2](https://doi.org/10.1175/1520-0485(1979)009h0189:MOHSIW2.0.CO;2)
- Goldberg, D. N., Gourmelen, N., Kimura, S., Millan, R., & Snow, K. (2019). How accurately should we model ice shelf melt rates? *Geophysical Research Letters*, 46, 189–199. <https://doi.org/10.1029/2018GL080383>
- Grobe, H., & Mackensen, A. (1992). Late Quaternary climatic cycles as recorded in sediments from the Antarctic continental margin. *Antarctic Research Series*, 56, 349–376. <https://doi.org/10.1029/AR056p0349>
- Hattermann, T. (2018). Antarctic thermocline dynamics along a narrow shelf with easterly winds. *Journal of Physical Oceanography*, 48(10), 2419–2443. <https://doi.org/10.1175/JPO-D-18-0064.1>
- Hattermann, T., Nøst, O. A., Lilly, J. M., & Smedsrud, L. H. (2012). Two years of oceanic observations below the Fimbul Ice Shelf, Antarctica. *Geophysical Research Letters*, 39, L12605. <https://doi.org/10.1029/2012GL051012>
- Hattermann, T., Smedsrud, L. H., Nøst, O. A., Lilly, J. M., & Galton-Fenzi, B. K. (2014). Eddy-resolving simulations of the Fimbul Ice Shelf cavity circulation: Basal melting and exchange with open ocean. *Ocean Modelling*, 82, 28–44. <https://doi.org/10.1016/j.ocemod.2014.07.004>
- Hellmer, H. H., Kauker, F., Timmermann, R., & Hattermann, T. (2017). The fate of the southern Weddell Sea continental shelf in a warming climate. *Journal of Climate*, 30(12), 4337–4350. <https://doi.org/10.1175/JCLI-D-16-0420.1>
- Heywood, K. J., Locarnini, R. A., Frew, R. D., Dennis, P. F., & King, B. A. (2013). Transport and water masses of the Antarctic Slope Front system in the eastern Weddell Sea. *Antarctic research series*, 75, 203–214. <https://doi.org/10.1029/AR075p0203>
- Hillenbrand, C.-D., Bentley, M. J., Stollard, T. D., Hein, A. S., Kuhn, G., Graham, A. G. C., et al. (2014). Reconstruction of changes in the Weddell Sea sector of the Antarctic Ice Sheet since the Last Glacial Maximum. *Quaternary Science Reviews*, 100, 111–136. <https://doi.org/10.1016/j.quascirev.2013.07.020>
- Hodgson, D. A., Hogan, K., Smith, J. M., Smith, J. A., Hillenbrand, C. D., Graham, A. G. C., et al. (2018). Deglaciation and future stability of the Coats Land ice margin, Antarctica. *The Cryosphere*, 12(7), 2383–2399. <https://doi.org/10.5194/tc-12-2383-2018>
- Hodgson, D. A., Jordan, T. A., De Rydt, J., Fretwell, P. T., Seddon, S. A., Becker, D., et al. (2019). Past and future dynamics of the Brunt Ice Shelf from seabed bathymetry and ice shelf geometry. *The Cryosphere*, 13(2), 545–556. <https://doi.org/10.5194/tc-13-545-2019>
- Hoppmann, M., Nicolaus, M., Paul, S., Hunkeler, P. A., Heinemann, G., Willmes, S., et al. (2015). Ice platelets below Weddell Sea landfast sea ice. *Annals of Glaciology*, 56(69), 175–190. <https://doi.org/10.3189/2015AoG69A678>
- Howat, I. M., Porter, C., Smith, B. E., Noh, M.-J., & Morin, P. (2019). The Reference Elevation Model of Antarctica. *The Cryosphere*, 13(2), 665–674. <https://doi.org/10.5194/tc-13-665-2019>

- IPCC (2019). IPCC Special Report on the Ocean and Cryosphere in a Changing Climate [H.-O. Pörtner, Roberts, D. C., Masson-Delmotte, V., Zhai, P., Tignor, M., Poloczanska, E., Mintenbeck, K., Nicolai, M., Okem, A., Petzold, J. Rama, B. Weyer, N. (eds.)]. Retrieved from <https://www.ipcc.ch/report/srocc/>
- Jenkins, A., Dutrieux, P., Jacobs, S. S., McPhail, S. D., Perrett, J. R., Webb, A. T., & White, D. (2010). Observations beneath Pine Island Glacier in West Antarctica and implications for its retreat. *Nature Geoscience*, 3(7), 468–472. <https://doi.org/10.1038/ngeo890>
- Kobarg (1988). The tide-dependent dynamics of the Ekstroem Ice Shelf, Antarctica. *Berichte zur Polar- und Meeresforschung*, 50, 1–164. [https://doi.org/10.2312/BzP\\_0050\\_1988](https://doi.org/10.2312/BzP_0050_1988)
- Kristoffersen, Y., Hofstede, C., Diez, A., Blenkner, R., Lambrecht, A., Mayer, C., & Eisen, O. (2014). Reassembling Gondwana: A new high quality constraint from vibroseis exploration of the sub-ice shelf geology of the East Antarctic continental margin. *Journal of Geophysical Research: Solid Earth*, 119, 9171–9182. <https://doi.org/10.1002/2014JB011479>
- Kuhn, G., & Gaedicke, C. (2015). A plan for interdisciplinary process, studies and geoscientific observations beneath the Eckstroem Ice Shelf (Sub-EIS-Obs). *Polarforschung*, 84(2), 99–102.
- Meijers, A. J. S., Meredith, M. P., Abrahamsen, E. P., Morales Maqueda, M. A., Jones, D. C., & Naveira Garabato, A. C. (2016). Wind-driven export of Weddell Sea slope water. *Journal of Geophysical Research: Oceans*, 121, 7530–7546. <https://doi.org/10.1002/2016JC011757>
- Meredith, M. P., Gordon, A. L., Naveira Garabato, A. C., Abrahamsen, E. P., Huber, B. A., Jullion, L., & Venables, H. J. (2011). Synchronous intensification and warming of Antarctic Bottom Water outflow from the Weddell Gyre. *Geophysical Research Letters*, 38, 7530–7546. <https://doi.org/10.1029/2010GL046265>
- Milillo, P., Rignot, E., Rizzoli, P., Scheuchl, B., Mouginot, J., Bueso-Bello, J., & Prats-Iraola, P. (2019). Heterogeneous retreat and ice melt of Thwaites Glacier, West Antarctica. *Science Advances*, 5(1), 1–8. <https://doi.org/10.1126/sciadv.aau3433>
- Morlighem, M., Rignot, E., Binder, T., Blankenship, D., Drews, R., Eagles, G., et al. (2020). Deep glacial troughs and stabilizing ridges unveiled beneath the margins of the Antarctic ice sheet. *Nature Geoscience*, 13(2), 132–137. <https://doi.org/10.1038/s41561-019-0510-8>
- Neckel, N., Drews, R., Rack, W., & Steinhage, D. (2012). Basal melting at the Ekström Ice Shelf, Antarctica, estimated from mass flux divergence. *Annals of Glaciology*, 53(60), 294–302. <https://doi.org/10.3189/2012AoG60A167>
- Nicholls, K. W., Abrahamsen, E. P., Buck, J. J. H., Dodd, P. A., Goldblatt, C., Griffiths, G., et al. (2006). Measurements beneath an Antarctic ice shelf using an autonomous underwater vehicle. *Geophysical Research Letters*, 33, L08612. <https://doi.org/10.1029/2006GL025998>
- Nøst, O. A. (2004). Measurements of ice thickness and seabed topography under the Fimbul Ice Shelf, Dronning Maud Land, Antarctica. *Journal of Geophysical Research*, 109, C10010. <https://doi.org/10.1029/2004JC002277>
- Nøst, O. A., Biuw, M., Tverberg, V., Lydersen, C., Hattermann, T., Zhou, Q., et al. (2011). Eddy overturning of the Antarctic Slope Front controls glacial melting in the Eastern Weddell Sea. *Journal of Geophysical Research*, 116, C11014. <https://doi.org/10.1029/2011JC006965>
- Padman, L., Erofeeva, S. Y., & Fricker, H. A. (2008). Improving Antarctic tide models by assimilation of ICESat laser altimetry over ice shelves. *Geophysical Research Letters*, 35, L22504. <https://doi.org/10.1029/2008GL035592>
- Paolo, F. S., Fricker, H. A., & Padman, L. (2015). Volume loss from Antarctic ice shelves is accelerating. *Science*, 348(6232), 327–331. <https://doi.org/10.1126/science.aaa0940>
- Patton, H., Swift, D. A., Clark, C. D., Livingstone, S. J., & Cook, S. J. (2016). Distribution and characteristics of overdeepenings beneath the Greenland and Antarctic ice sheets: Implications for overdeepening origin and evolution. *Quaternary Science Reviews*, 148, 128–145. <https://doi.org/10.1016/j.quascirev.2016.07.012>
- Pattyn, F., Favier, L., Sun, S., & Durand, G. (2017). Progress in numerical modeling of Antarctic ice-sheet dynamics. *Current Climate Change Reports*, 3(3), 174–184. <https://doi.org/10.1007/s40641-017-0069-7>
- Pritchard, H. D., Ligtenberg, S. R. M., Fricker, H. A., Vaughan, D. G., Van Den Broeke, M. R., & Padman, L. (2012). Antarctic ice-sheet loss driven by basal melting of ice shelves. *Nature*, 484(7395), 502–505. <https://doi.org/10.1038/nature10968>
- Rignot, E., Jacobs, S., Mouginot, J., & Scheuchl, B. (2013). Ice-shelf melting around Antarctica. *Science*, 341(6143), 266–270. <https://doi.org/10.1126/science.1235798>
- Ritz, C., Edwards, T. L., Durand, G., Payne, A. J., Peyaud, V., & Hindmarsh, R. C. A. (2015). Potential sea-level rise from Antarctic ice-sheet instability constrained by observations. *Nature*, 528(7580), 115–118. <https://doi.org/10.1038/nature16147>
- Smetacek, V., Scharek, R., Gordon, L. I., Eicken, H., Fahrback, E., Rohardt, G., & Moore, S. (1992). Early spring phytoplankton blooms in ice platelet layers of the southern Weddell Sea, Antarctica. *Deep Sea Research Part A, Oceanographic Research Papers*, 39(2), 153–168. [https://doi.org/10.1016/0198-0149\(92\)90102-Y](https://doi.org/10.1016/0198-0149(92)90102-Y)
- Sun, S., Hattermann, T., Pattyn, F., Nicholls, K. W., Drews, R., & Berger, S. (2019). Topographic shelf waves control seasonal melting near Antarctic Ice Shelf grounding lines. *Geophysical Research Letters*, 46, 9824–9832. <https://doi.org/10.1029/2019GL083881>
- Thompson, A. F., Stewart, A. L., Spence, P., & Heywood, K. J. (2018). The Antarctic Slope Current in a changing climate. *Reviews of Geophysics*, 56, 741–770. <https://doi.org/10.1029/2018RG000624>
- Timmermann, R., & Hellmer, H. H. (2013). Southern Ocean warming and increased ice shelf basal melting in the twenty-first and twenty-second centuries based on coupled ice-ocean finite-element modelling. *Ocean Dynamics*, 63(9–10), 1011–1026. <https://doi.org/10.1007/s10236-013-0642-0>
- Tinto, K. J., Padman, L., Siddoway, C. S., Springer, S. R., Fricker, H. A., Das, I., et al. (2019). Ross Ice Shelf response to climate driven by the tectonic imprint on seafloor bathymetry. *Nature Geoscience*, 12(6), 441–449. <https://doi.org/10.1038/s41561-019-0370-2>
- Zhou, Q., Hattermann, T., Nøst, O. A., Biuw, M., Kovacs, K. M., & Lydersen, C. (2014). Wind-driven spreading of fresh surface water beneath ice shelves in the Eastern Weddell Sea. *Journal of Geophysical Research: Oceans*, 119, 3818–3833. <https://doi.org/10.1002/2013JC009556>